Formation Mechanism of $CaO-SiO_2-Al_2O_3-(MgO)$ Inclusions in Si-Mn-Killed Steel with Limited Aluminum Content During the Low Basicity Slag Refining

KUNPENG WANG, MIN JIANG, XINHUA WANG, YING WANG, HAOQIAN ZHAO, and ZHANMIN CAO

Pilot trails were carried out to study the formation mechanism of $CaO-SiO_2-Al_2O_3-(MgO)$ inclusions in tire cord steel. 48 samples were taken from 8 heats of liquid steel during secondary refining, which were subsequently examined by an automatic scanning electron microscope with energy dispersive spectrometer (SEM–EDS). Characteristics of thousands of oxide inclusions at different refining stages were obtained, including their compositions, sizes, morphologies, *etc*. Based on the obtained information of inclusions, details during formation of $CaO-SiO_2-Al_2O_3-(MgO)$ inclusions were revealed and a new mechanism was proposed, including their origin, formation, and evolution during the refining process. It was found that $CaO-SiO_2-Al_2O_3-(MgO)$ inclusions were initially originated from the $CaO-SiO_2-MnO-(MgO)$ inclusions, which were formed during BOF tapping by the coalescence between $MnO-SiO_2$ deoxidation products and the emulsified slag particles because of violent flow of steel. This can be well confirmed by the evaluation of the formation thermodynamics of $CaO-SiO_2-MnO-(MgO)$ inclusions, which was proved very difficult to be produced by intrinsic reactions inside liquid steel. Because of chemical reactions between $CaO-SiO_2-MnO-(MgO)$ inclusions and molten steel, they were mainly changed into $CaO-SiO_2-MnO-Al_2O_3-(MgO)$ and partially into $CaO-SiO_2-Al_2O_3-(MgO)$, which may be detrimental to the cold drawing ability of coils. Based on this finding, improvements were made in industrial production during BOF tapping and secondary refining. The results indicated that such $(CaO-SiO_2)$-based inclusions existed in conventional process were effectively decreased after the improvements.

DOI: 10.1007/s11663-015-0502-z

I. INTRODUCTION

STEEL rods for tire cords and saw wires are designed for higher tensile properties and drawn into ever smaller diameters. A crucial issue of these wires is the breakages during fabrication, which were mainly caused by non-metallic inclusions as shown in many researches.[1–3] Since inclusions can act as crack initiation sites in the wires when subjected to cold drawing and cyclic stress, it would be more appreciated if they were with small size, decreased quantity, and good deformability. It is known that deformability of inclusions is affected by the melting points of themselves, which in turn closely related to their own chemistry.[4,5] Therefore, inclusions, such as alumina which is higher in melting point and hardness, should be avoided. As a result, Si-Mn complex deoxidation combined with low basicity top slag refining is generally used to produce tire cord steel for improved deformation of inclusions.

Commonly, inclusions in tire cord steel can be roughly classified into two categories. One type is composed of $MnO-SiO_2-Al_2O_3$ system. While the other kind is $CaO-SiO_2-Al_2O_3$, usually together with some MgO and sometimes also MnO.[6–8] It is generally held that best deformability of these inclusions can be expected if they contained about 20 wt pct Al_2O_3. Many researchers studied the effect of top slag on the composition of inclusions by either experiments or thermodynamic predictions.[6–17] To targeted this optimal Al_2O_3 content in inclusions, slag with basicity about 1.0 and Al_2O_3 about 8 wt pct was proved to be fine.[7] Under this circumstance, the optimum dissolved aluminum in steel would be about 0.0004 wt pct.

As far as the formation mechanisms of these two kinds of inclusions, $MnO-SiO_2-Al_2O_3$ inclusions are widely accepted as deoxidation products.[9–15] However, there are still some controversies over the origins of $CaO-SiO_2-Al_2O_3-(MgO)$ inclusions. Some researchers[7,8] suggested that $CaO-SiO_2-Al_2O_3-(MgO)$ inclusions were entrapped slag particles. Whereas other

KUNPENG WANG, Ph.D. Student, MIN JIANG, Assistant Professor, XINHUA WANG, Professor, and ZHANMIN CAO, Associate Professor, are with the School of Metallurgical and Ecological Engineering, University of Science and Technology Beijing, Beijing 100083, P.R. China. Contact e-mail: jiangmin@ustb.edu.cn YING WANG, Dr./Engineer, and HAOQIAN ZHAO, Engineer, are with the Xingtai Iron and Steel Corp., Ltd., Hebei 054027, P.R. China.
Manuscript submitted September 21, 2015.
Article published online November 4, 2015.

studies[14,16] reported that these CaO-containing inclusions were originated from interaction of the molten steel reacted with top slag in a ladle. Nevertheless, both two points of views cannot perfectly explain the findings in practice. For instance, Al_2O_3 content is usually higher in CaO-SiO_2-Al_2O_3-(MgO) inclusions than that in top slag. Moreover, CaO-SiO_2-Al_2O_3-(MgO) inclusions always contain a small amount of MgO, whereas MnO-SiO_2-Al_2O_3 system inclusions can be free of MgO.[16] Besides, Ca content in liquid steel is usually low and can be less than 0.0001 wt pct.[18] Therefore, formation thermodynamics of CaO-SiO_2-Al_2O_3-(MgO) system inclusions by intrinsic reactions inside liquid steel under such low Ca content should be checked. As it is known, CaO-SiO_2-Al_2O_3-(MgO) system inclusions are frequently reported as the reason of wire breakages because of poor deformability during cold drawing.[6,19,20] Therefore, clarification of their formation mechanism in tire cord steel should be further specified.

Based on this consideration, industry trials were carried out in the steel plant. The results showed that only a few CaO-SiO_2-Al_2O_3 ternary inclusions were observed in steel during refining and most of them always contain some MnO and MgO, existing as quaternary or quinary system. Furthermore, CaO-SiO_2-MnO-(MgO) inclusions and CaO-SiO_2-(MgO) inclusions which were seldom reported in previous literatures were also found after BOF tapping. Therefore, different from previous studies, attentions were paid by present authors to the origin and evolution of CaO-SiO_2-MnO-(MgO) inclusions. And a new formation mechanism of CaO-SiO_2-Al_2O_3-(MgO) inclusions was proposed on the basis of experimental findings and thermodynamic analysis.

II. EXPERIMENTS

A. *Experiment and Samplings*

Industrial trials were carried out in a steel plant for tire cord steel. The steelmaking process was featured by "BOF (Basic Oxygen Furnace) → LF (Ladle Furnace) refining → Bloom casting." During BOF tapping, Fe-Si alloy and Fe-Mn alloy with low aluminum as well as synthetic slag were added into molten steel for deoxidization, alloying, and early slag formation. Low basicity slag (CaO/SiO_2: 0.8 to 1.0) was used during LF refining together with argon bottom blowing at a proper stirring energy to prevent exposure of liquid steel to the air. Soft blowing by argon gas was employed after LF refining for better removal of inclusions. In the experiments, 48 liquid steel samples were taken from 8 heats by bucket-shaped samplers. Sampling scheme of each heat is schematically shown in Figure 1.

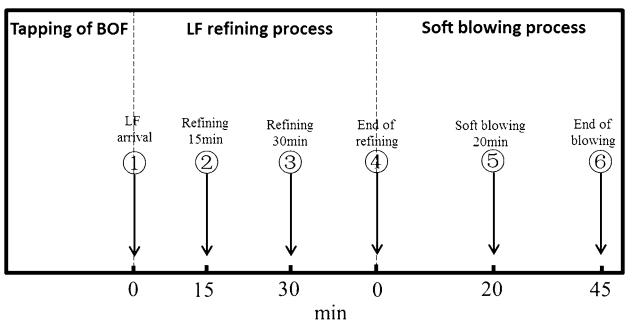

Fig. 1—Sampling scheme of refining process.

B. *Analysis of Samples*

Steel and slag samples were prepared for chemical analysis. Acid-soluble Al, Ca, and Mg contents in steel were analyzed by ICP-MS (inductive couple plasma-mass spectrometry) method. Slag composition was analyzed by an X-ray fluorescence spectrometer. Analyzed compositions of steel and slag are shown in Tables I and II, respectively. All the obtained steel samples were ground and mirror polished for inclusion inspection under an automatic SEM with EDS named ASPEX PSEM eXplorer. Details of this equipment have been described in one of the authors' previous paper.[21] Inclusions within 1 μm were not taken into account during the detection. Characteristics of thousands of oxide inclusions in different refining stages were obtained, including composition, size, and morphology.

III. RESULTS AND DISCUSSION

A. *Classification of Inclusions*

4933 oxide inclusions were totally examined in all the 48 samples. Figure 2 showed the relationship between contents of MgO and CaO in these inclusions. Figure was divided into four regions by line L_1 (L_1 represents CaO = 9.5 wt pct) and line L_2 (L_2 represents MgO = 1.0 wt pct). Number of inclusions in each region was labeled at the top-left corner. It can be seen that 1036 and 3826 inclusions distributed in regions II and III, respectively, accounting for a percentage of 98.6 pct of all inclusions. Particularly, 98.7 pct of the inclusions in regions I and III (with CaO < 9.5 wt pct) were free of MgO. On the contrary, 97.9 pct of the inclusions located in regions II and IV (with CaO > 9.5 wt pct) were MgO containing. Thus, these inclusions were classified into two categories. The first group is MgO-containing mainly in region II, while the other is MgO free mainly located in region III.

Content of each component in these two kinds of inclusions are plotted in Figure 3. It can be seen that MgO-free inclusions were mainly composed of MnO and SiO_2 while Al_2O_3 contents in them scattered around 10 wt pct. Therefore, MgO-free inclusions can be classified into two subcategories according to their Al_2O_3 contents, named MnO-SiO_2 system (with Al_2O_3 < 10 pct) and MnO-SiO_2-Al_2O_3 system (with Al_2O_3 > 10 pct), respectively. As for MgO-containing inclusions, CaO and SiO_2 are the main components while MgO was less than 10 wt pct. Contents of Al_2O_3 and MnO in them varied around 10 wt pct. According to the contents of Al_2O_3 and MnO, MgO-containing inclusions can be divided into four subcategories:

Table I. Chemical Compositions of Steel Samples at Different Stages (Wt Percent)

Stage	C	Si	Mn	S	Als	Ca	Mg
After BOF tapping	0.77	0.18	0.46	0.0070	0.0003	<0.0002	<0.0002
End of LF refining	0.83	0.20	0.51	0.0072	0.0006	<0.0002	<0.0002
End of blowing	0.83	0.21	0.51	0.0072	0.0007	<0.0002	<0.0002

Table II. Chemical Compositions of Slag Samples at Different Stages (Wt Percent)

Stage	CaO	MgO	MnO	SiO_2	Al_2O_3	FeO	CaO/SiO_2
After BOF tapping	32.8	8.0	4.3	44.6	2.9	2.6	0.74
End of LF refining	38.9	10.5	2.5	37.9	7.5	1.5	1.03
End of blowing	38.0	11.4	1.8	38.7	7.8	1.0	0.98

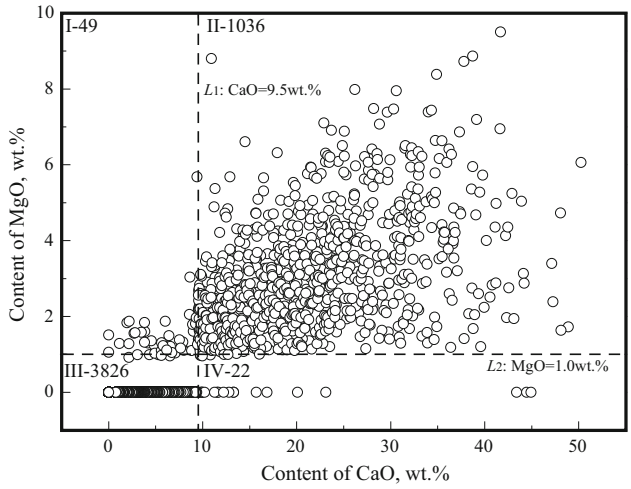

Fig. 2—Relationship between contents of MgO and CaO in inclusions.

$CaO-SiO_2$-(MgO) system, $CaO-SiO_2$-MnO-(MgO) system, $CaO-SiO_2-Al_2O_3$-(MgO) system, and $CaO-SiO_2-MnO-Al_2O_3$-(MgO) system. Standard for classification of inclusions is shown in Figure 4. It can be seen that MgO-containing inclusions were always ($CaO-SiO_2$)-based, while MgO-free inclusions always contained very limited amount of CaO.

B. *Evolution of Inclusions During Secondary Refining Process*

1. *Morphologies and sizes of inclusions*

Morphologies of typical MgO-free inclusions can be read from Figure 5. $MnO-SiO_2$ system inclusions can be observed from the samples after deoxidation and $MnO-SiO_2-Al_2O_3$ system inclusions can be found from the end of LF refining till the end of soft blowing. All these inclusions were globular, which implied that they were in liquid state at steelmaking temperature [1853 K (1580 °C)]. Both of the two types of inclusions were mainly in small size less than 3 μm.

Typical MgO-containing inclusions are presented in Figure 6. $CaO-SiO_2$-(MgO) system inclusions in Figures 6(a) through (c) and $CaO-SiO_2$-MnO-(MgO) system inclusions in Figures 6(d) through (f) were observed in samples just after BOF tapping. Al_2O_3 content in $CaO-SiO_2$-MnO-(MgO) inclusions in Figures 6(g) and (h) showed a rise after 30 minutes refining. $CaO-SiO_2-Al_2O_3$-MnO-(MgO) system inclusions in Figure 6(i) and $CaO-SiO_2-Al_2O_3$-(MgO) system inclusions in Figure 6(j) can be found from the end of LF refining till the end of soft blowing. These MgO-containing inclusions were quite different in size. $CaO-SiO_2$-(MgO) system inclusions were the largest and mainly in several tens or even hundreds of microns, while $CaO-SiO_2$-MnO-(MgO), $CaO-SiO_2-Al_2O_3$-(MgO), and $CaO-SiO_2-MnO-Al_2O_3$-(MgO) system inclusions were only in several microns. Particularly, it can be seen from Figures 5 and 6 that MgO-containing inclusions were obviously larger than MgO-free ones.

2. *Changes in ratios of each kind of inclusion*

Figure 7 showed changes in the ratios of each kind of inclusion at different stages. It can be seen that inclusions at the beginning of LF refining were mainly $MnO-SiO_2$ and $CaO-SiO_2$-MnO-(MgO), taking a percentage of 87 and 12 pct, respectively. By contrast, $MnO-SiO_2-Al_2O_3$ and $CaO-SiO_2-Al_2O_3$-based inclusions only occupied very low fractions. Ratios of each kind of inclusions maintained very steady but it changed dramatically after 30 minutes of ladle refining. It can be seen clearly that fraction of $MnO-SiO_2-Al_2O_3$ inclusions increased sharply against with the obvious decrease of $MnO-SiO_2$ inclusions, while $CaO-SiO_2-MnO-Al_2O_3$-(MgO), and $CaO-SiO_2-Al_2O_3$-(MgO) indicated a rise with the decreased ratio of $CaO-SiO_2$-MnO-(MgO) and $CaO-SiO_2$-(MgO) inclusions. Similarity in the chemistry changes of all these inclusions was the rise of Al_2O_3 contents after enough long time of refining. Increase of Al_2O_3 in inclusions reached a plateau after 20 minutes' soft blowing, with complete disappearance of $MnO-SiO_2$ and $CaO-SiO_2$-MnO-(MgO) inclusions. This phenomenon was attributed to the continuous chemical reactions among slag-steel inclusions. As a result, at the end of soft blowing, $MnO-SiO_2-Al_2O_3$ system inclusions and $CaO-SiO_2-Al_2O_3$-MnO-(MgO) system inclusions accounted for 83 and 15 pct of all the observed particles, respectively. Based on the analysis of changes in ratios of inclusions, it was reasonably concluded that $MnO-SiO_2-Al_2O_3$ inclusions were originated from $MnO-SiO_2$ inclusions, while $CaO-SiO_2-MnO-Al_2O_3$-(MgO) and

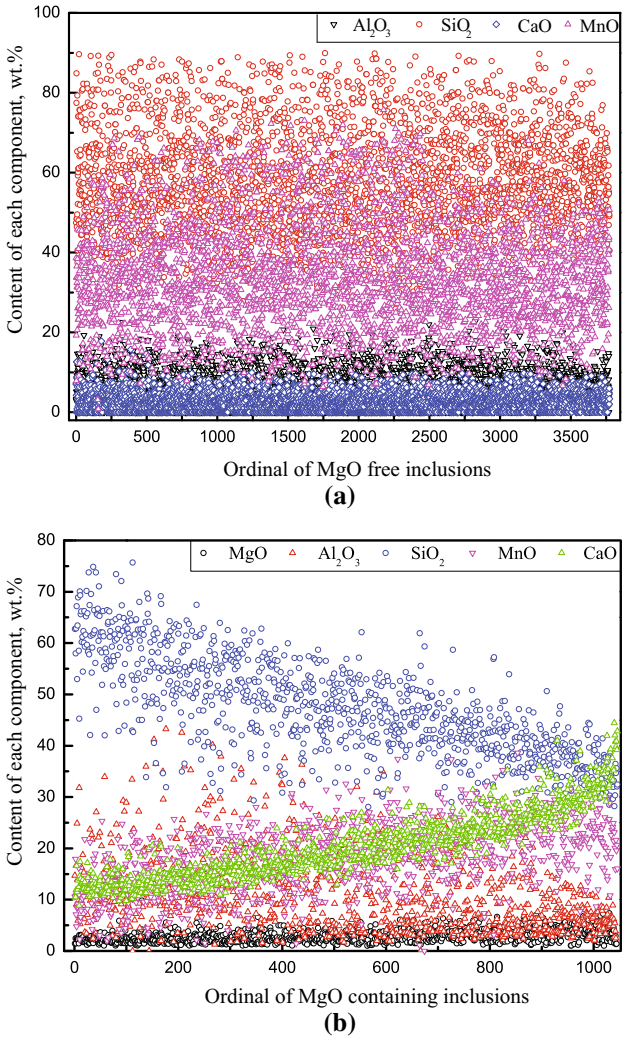

Fig. 3—Content of each component in: (*a*) MgO-free inclusions and (*b*) MgO-containing inclusions.

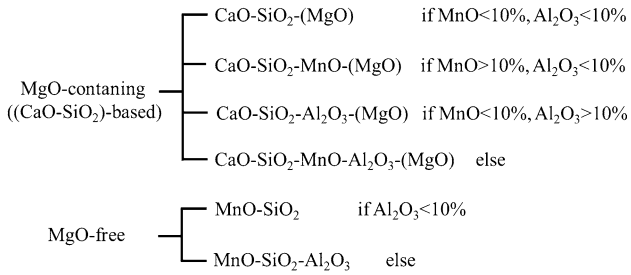

Fig. 4—Standard for classification of inclusions.

$CaO\text{-}SiO_2\text{-}Al_2O_3\text{-}(MgO)$ inclusions were evolved from $CaO\text{-}SiO_2\text{-}MnO\text{-}(MgO)$ inclusions.

3. *Changes in chemical composition of inclusions*

Figure 8 gives the average content of each component in MgO-free inclusions. Content of CaO showed constant low levels during the whole process. Content of SiO_2 and MnO initially fluctuated in the first 30 minutes of LF refining, which may due to the composition adjustment operation by adding alloys. However, SiO_2 and MnO in them declined gradually and continuously afterward, while Al_2O_3 showed an increasing tendency against the refining time. After 20 minutes soft blowing, content of each component in inclusions become stable and Al_2O_3 increased to 17 wt pct, which corresponded to the above-mentioned evolution of $MnO\text{-}SiO_2$ inclusions into $MnO\text{-}SiO_2\text{-}Al_2O_3$ system inclusions due to the rise of Al_2O_3.

Figure 9 shows the average content of each component in MgO-containing inclusions. However, content of MgO remained at a level of only 3 to 4 wt pct during the whole process. MnO, SiO_2, and CaO generally indicated declining trends against process time. Al_2O_3 content in inclusions was also low in the initial 30 minutes but showed a significant increase at the end of LF refining. The above-mentioned changes of $CaO\text{-}SiO_2\text{-}MnO\text{-}(MgO)$ inclusions into $CaO\text{-}SiO_2\text{-}MnO\text{-}Al_2O_3\text{-}(MgO)$ inclusions and $CaO\text{-}SiO_2\text{-}Al_2O_3\text{-}(MgO)$ inclusions occurred.

From the analysis above, it is known $CaO\text{-}SiO_2\text{-}Al_2O_3\text{-}(MgO)$ inclusions were originated from $CaO\text{-}SiO_2\text{-}MnO\text{-}(MgO)$ inclusions. As a result, more detailed information of the latter would be helpful for more effective control of the former. In order to confirm the time period of $CaO\text{-}SiO_2\text{-}MnO\text{-}(MgO)$ inclusions formation, samples taken at the endpoint of BOF were first examined but no inclusions were observed. Impressively, $CaO\text{-}SiO_2\text{-}MnO\text{-}(MgO)$ inclusions were detected in the sample picked after BOF tapping, as shown in Figure 9. Therefore, it can be reasonably to confirm that $CaO\text{-}SiO_2\text{-}MnO\text{-}(MgO)$ inclusions was caused during BOF tapping.

C. *Thermodynamic Considerations*

In order to confirm whether $CaO\text{-}SiO_2\text{-}MnO\text{-}(MgO)$ can be produced by intrinsic chemical reactions inside liquid steel during BOF tapping, thermodynamic calculation was performed using Factsage6.4 at 1853 K (1580 °C). Ftoxide (for oxides) and FSStel (for liquid steel) solution databases were employed in Factsage6.4 Equilib module. Figure 10 showed the calculated amount of liquid inclusion and each component in inclusions that equilibrated with Fe-0.77C-0.46Mn-0.18Si-0.0070S-0.0500O-0.0003Al-*x*Ca system liquid steel. When Ca content in liquid steel was less than 0.0010 wt pct, liquid inclusions were $MnO\text{-}SiO_2$ system containing very small amount of CaO and Al_2O_3, which agreed with the experimental results. Weight percentages of CaO in liquid inclusion increased with the rise of Ca in liquid steel. It has been known from above section that average content of CaO in $CaO\text{-}SiO_2\text{-}MnO\text{-}(MgO)$ inclusions at the beginning of LF was about 20 wt pct. In this case, it can be seen that the corresponded content of Ca in liquid steel should not less than 0.0147 wt pct. However, contents of Ca in liquid steel bulk were less than 0.0002 wt pct. Additionally, local enrichment of Ca in molten steel cannot occur because of no Ca was

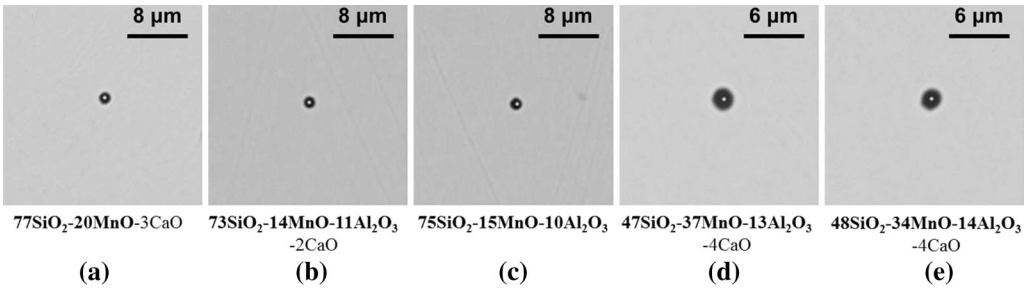

Fig. 5—Typical MgO-free inclusions, (*a*) MnO-SiO_2 system, (*b* through *e*) MnO-SiO_2-Al_2O_3 system.

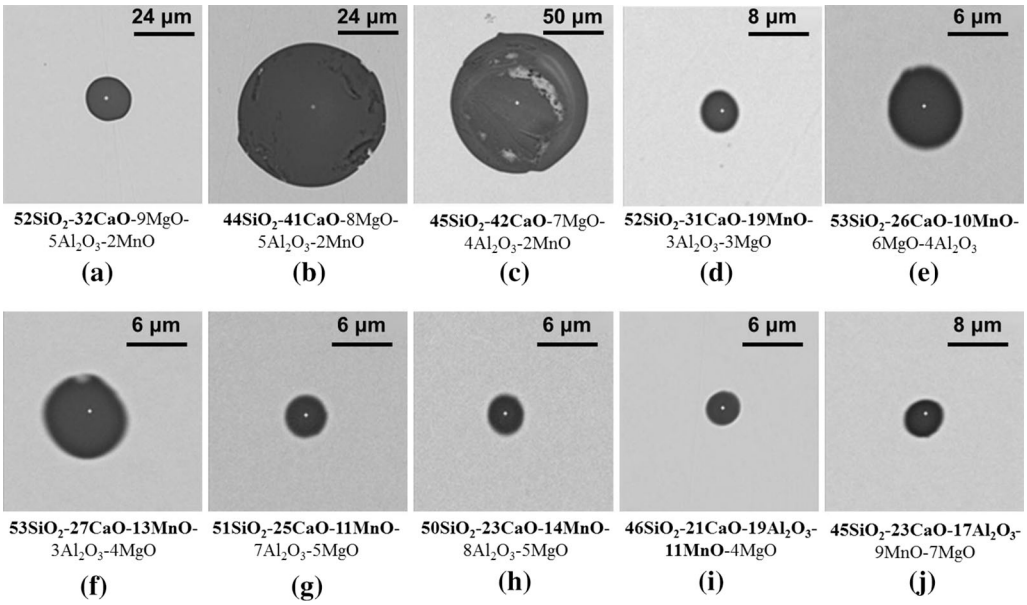

Fig. 6—Typical MgO-containing inclusions, (*a* through *c*) CaO-SiO_2-(MgO) system, (*d* through *h*) CaO-SiO_2-MnO-(MgO) system, (*i*) CaO-SiO_2-MnO-Al_2O_3-(MgO) system, (*j*) CaO-SiO_2-Al_2O_3-(MgO) system.

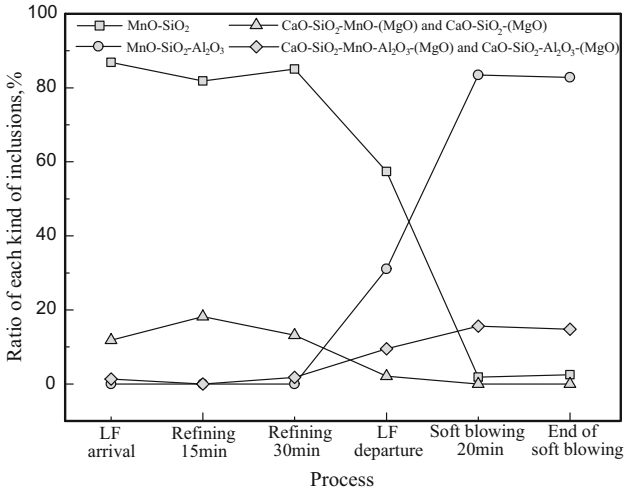

Fig. 7—Changes in the ratios of each kind of inclusions at different stages.

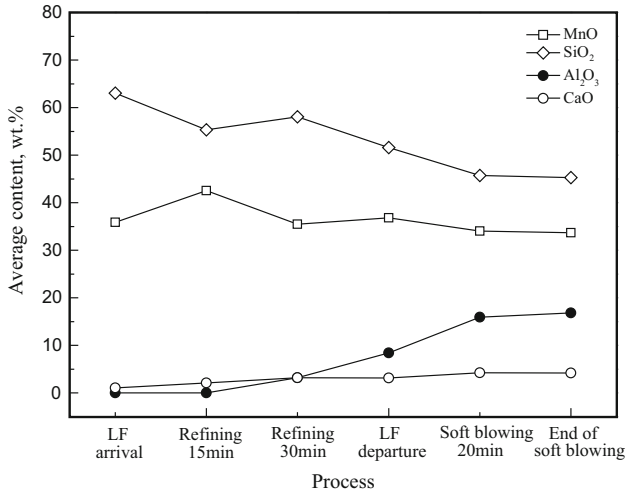

Fig. 8—Average content of each component in MgO-free inclusions at different stage.

added during refining. Therefore, it is concluded that CaO-SiO_2-MnO-(MgO) inclusions were exogenous particles caused during BOF tapping.

Composition of MnO-SiO_2, CaO-SiO_2-(MgO), and CaO-SiO_2-MnO-(MgO) inclusions observed in the samples taken at BOF tapping were projected into

$CaO-SiO_2$-MnO ternary system with the reference of top slag composition, as shown in Figure 11. Unlike $MnO-SiO_2$ inclusions produced in deoxidation, $CaO-SiO_2$-(MgO) inclusions and $CaO-SiO_2$-MnO-(MgO) inclusions always contained a small amount of MgO. Composition of $CaO-SiO_2$-(MgO) system inclusions was similar to the top slag. Moreover, from above Figures 6(a) through (c), it has known that most of the $CaO-SiO_2$-(MgO) inclusions were with sizes of dozens microns or even hundreds of microns. Therefore, $CaO-SiO_2$-(MgO) system inclusions were concluded as the entrapped slag particles. By comparison, $CaO-SiO_2$-MnO-(MgO) inclusions contained more CaO than $MnO-SiO_2$ while more MnO than top slag. In addition, size of $CaO-SiO_2$-MnO-(MgO) inclusions was larger than $MnO-SiO_2$ inclusions, while smaller than $CaO-SiO_2$-(MgO) inclusions. If line *l* was drawn to connect the average composition of $MnO-SiO_2$ inclusions and top slag, it can be seen most $CaO-SiO_2$-MnO-(MgO) inclusions were concentrated around this line. Hence, a reasonable explanation can be proposed that $CaO-SiO_2$-MnO-(MgO) was the coalescence product of $MnO-SiO_2$ inclusions and entrapped slag particles.

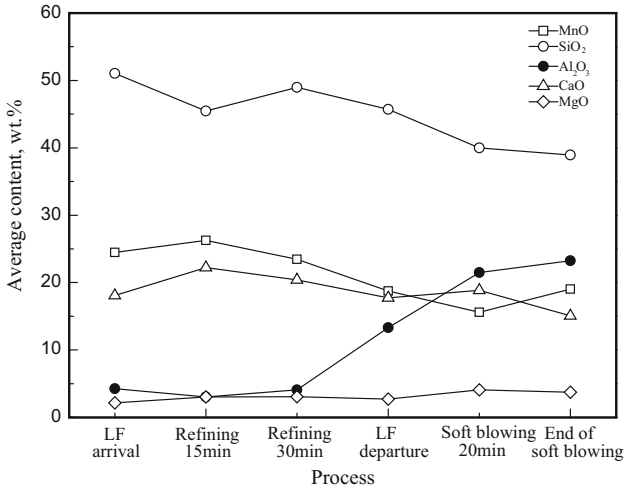

Fig. 9—Average content of each component in MgO-containing inclusions at different stage.

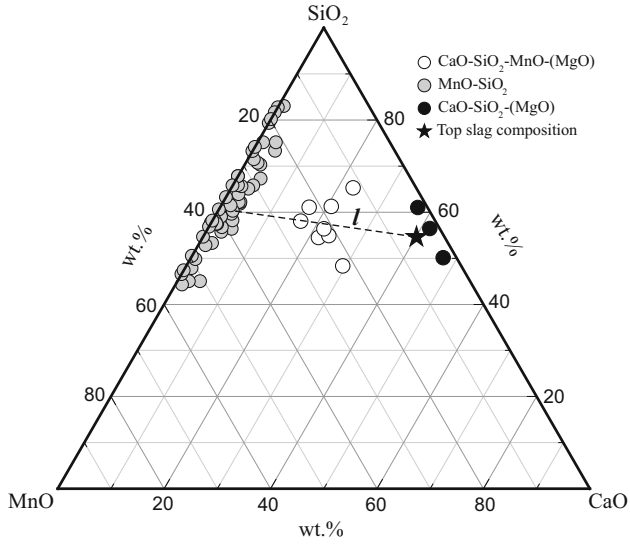

Fig. 11—Composition distribution of inclusions observed after tapping of BOF with the comparison of top slag.

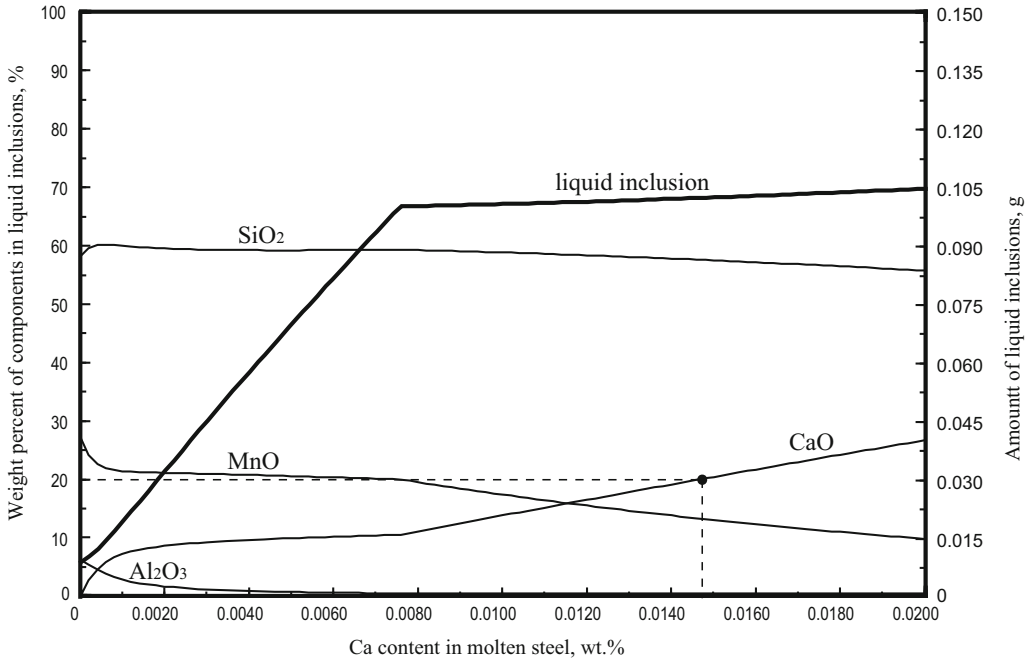

Fig. 10—Amount of liquid inclusion and predicted content of each component equilibrated with Fe-0.77C-0.46Mn-0.18Si-0.0070-S-0.0500O-0.0003Al-*x*Ca steel at 1853 K (1580 °C).

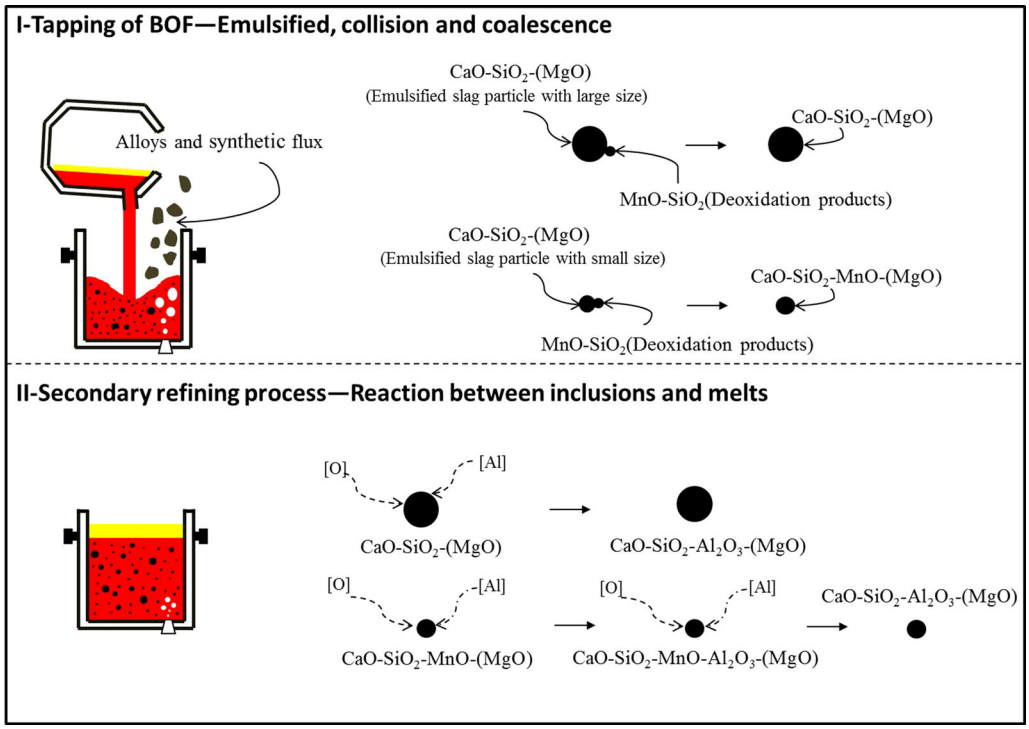

Fig. 12—Schematic diagram of formation mechanism of $CaO-SiO_2-Al_2O_3-(MgO)$ inclusions.

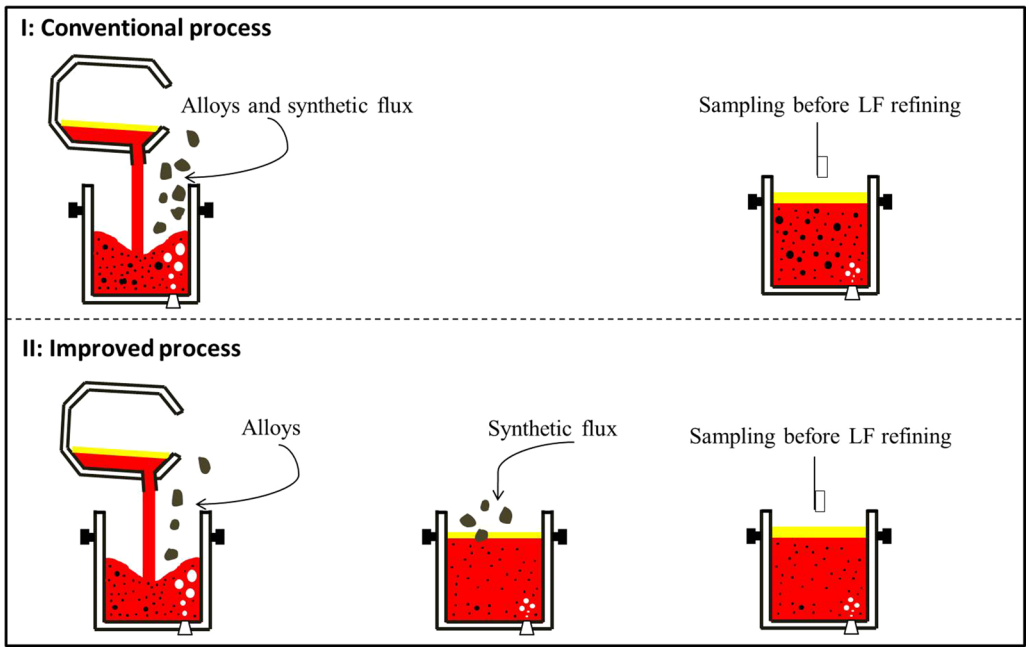

Fig. 13—Sampling scheme of conventional process and improved process.

D. *Explanation on the Origin and Evolution of $CaO-SiO_2-MnO-(MgO)$ System Inclusions*

With the addition of Fe-Si alloy and Fe-Mn alloy-contained low aluminum together with synthetic flux into molten steel during BOF tapping, alloys would quickly dissolve and react with dissolved oxygen. As a result, $MnO-SiO_2$ inclusions would be largely produced. Simultaneously, emulsification of the added synthetic flux in liquid steel can be expected because of strong agitation of the liquid steel tapping flow, resulting in the formation of exogenous inclusions. As shown in Figure 12, the emulsified slag particles and $MnO-SiO_2$

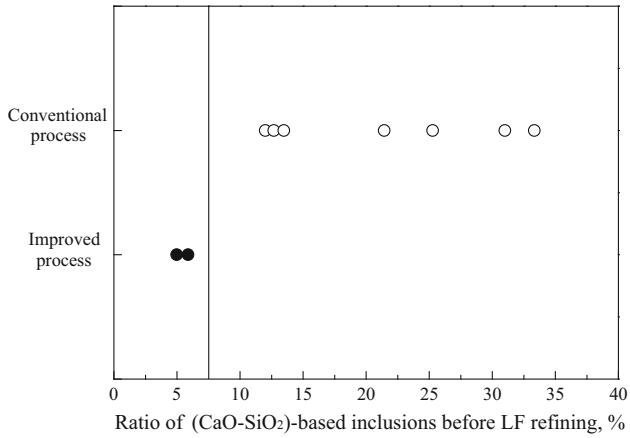

Fig. 14—Changes in the ratio of ($CaO-SiO_2$)-based inclusions before LF refining in conventional/improved process.

inclusions can frequently collide and coalescence with each other because of the violent agitation of steel flow. As a result, composition of the emulsified slag particles can be changed after collide and coalescence. If they were with larger sizes, changes of compositions would be more negligible and vice versa. And these small-sized emulsified particles would be changed into $CaO-SiO_2-MnO-(MgO)$ inclusions, while those large-sized ones would be remain as $CaO-SiO_2-(MgO)$ inclusions, which accounted why the former was always detected in smaller sizes, while the latter in larger sizes during the experiments.

With the proceeding of the refining process, content of acid-soluble Al in liquid steel gradually increased due to addition of alloys and also the chemical reactions between steel and slag. Content of Al_2O_3 in inclusions would be increased because of the chemical reactions between inclusions and liquid steel. As a result, $MnO-SiO_2$ evolved into $MnO-SiO_2-Al_2O_3$ inclusions, while $CaO-SiO_2-MnO-(MgO)$ evolved into $CaO-SiO_2-MnO-Al_2O_3-(MgO)$ inclusions. If acid-soluble Al in liquid steel was high enough and reaction time was sufficient, $CaO-SiO_2-MnO-Al_2O_3-(MgO)$ would be further transformed into $CaO-SiO_2-Al_2O_3-(MgO)$ inclusions. Most of the $CaO-SiO_2-(MgO)$ system inclusions with large size would be floated out of liquid steel easier and the remained ones were changed into $CaO-SiO_2-Al_2O_3-(MgO)$ inclusions. This formation and evolution mechanism can also explained the existence of MgO in ($CaO-SiO_2$)-based inclusions.

E. *Improvements in Industrial Production*

From the analysis above, it can be seen that strong agitation is the direct reason of slag emulsion into molten steel, resulting in the formation of ($CaO-SiO_2$)-based inclusions. Thus, improvements were made in industrial production, as schematically shown in Figure 13. In the conventional process, alloys and synthetic flux were added into molten steel during tapping. However, in the improved process, alloys and synthetic flux were dividedly added. During BOF tapping, only alloys were added while the synthetic flux was added afterward. Totally 9 heats of pilot trials were carried out, of which 7 was with conventional process and the other 2 was with the new process. Steel samples were taken by the bucket samplers before LF refining, which were subjected to observation of inclusions by the ASPEX eXplorer and about 100 oxide inclusions were analyzed in each sample.

Figure 14 gives the ratio of ($CaO-SiO_2$)-based inclusions in each sample. It can be seen that this ratio varied in the range of 12 to 33 pct with an average of 21 pct in the conventional process while this ratio was sharply decreased to 6 pct in the improved process. Cramb and Byrne confirmed that slag carryover from the BOF into the ladle was a potential source of exogenous inclusion by slag tracer experiment.[22,23] According to their study results, the ($CaO-SiO_2$)-based inclusions observed in improved process may originate from the slag which carryover from the BOF into the ladle, although great care was taken to ensure slag-free tapping in practical operation.

IV. CONCLUSIONS

In current study, formation of $CaO-SiO_2-Al_2O_3-(MgO)$ complex inclusions were examined and reevaluated in a more detailed way. Large scale of samplings was carried out from BOF tapping till the end of secondary refining for 8 heats of molten steel in industrial production. By analyzing the types, sizes, compositions, and morphology of inclusions, continuous changes of inclusions at different stages of the whole process can be depicted. And a new mechanism was proposed to explain the formation of $CaO-SiO_2-Al_2O_3-(MgO)$ inclusions. Moreover, improvements were made to industrial production, which effectively decreased the amount of such detrimental complex inclusions. Important findings can be concluded as following:

(1) Inclusions during secondary refining can be divided into two kinds, that is, MgO-containing inclusions and MgO-free inclusions. The former was always ($CaO-SiO_2$)-based, including $CaO-SiO_2-(MgO)$, $CaO-SiO_2-MnO-(MgO)$, $CaO-SiO_2-MnO-Al_2O_3-(MgO)$, and $CaO-SiO_2-Al_2O_3-(MgO)$. While MgO-free inclusions were mainly $MnO-SiO_2$ and $MnO-SiO_2-Al_2O_3$ with very limited CaO.
(2) $CaO-SiO_2-Al_2O_3-(MgO)$ and $CaO-SiO_2-MnO-Al_2O_3-(MgO)$ inclusions were originated from $CaO-SiO_2-MnO-(MgO)$ inclusions, which were formed during BOF tapping. While $MnO-SiO_2$ inclusions produced during Si-Mn deoxidation were the origins of $MnO-SiO_2-Al_2O_3$ inclusions that largely existed during ladle refining.
(3) Thermodynamic calculation showed that $CaO-SiO_2-MnO-(MgO)$ inclusions can hardly be formed by intrinsic chemical reactions in liquid steel because Ca content in steel was too low. They were produced by collisions and coalescences between $MnO-SiO_2$ inclusions and emulsified top slag particles.

(4) Formation of $CaO\text{-}SiO_2\text{-}Al_2O_3\text{-}(MgO)$ and $CaO\text{-}SiO_2\text{-}MnO\text{-}Al_2O_3\text{-}(MgO)$ inclusions involved two important steps. First, emulsion of slag occurred during BOF tapping, resulting in the entrapment of slag particles. Collisions and coalescences between these exogenous particles and $MnO\text{-}SiO_2$ inclusions happened because of violent flow of molten steel. Second, $CaO\text{-}SiO_2\text{-}MnO\text{-}(MgO)$ inclusions reacted with molten steel, causing the increase of Al_2O_3 in inclusions and resulting in the evolution of $CaO\text{-}SiO_2\text{-}MnO\text{-}(MgO)$ into $CaO\text{-}SiO_2\text{-}MnO\text{-}Al_2O_3\text{-}(MgO)$ and $CaO\text{-}SiO_2\text{-}Al_2O_3\text{-}(MgO)$ system inclusions.

(5) Improved process remarkably reduced the existence of $(CaO\text{-}SiO_2)$-based inclusions by adding synthetic flux without strong agitation, which would effectively improve the quality of products. This result also powerfully verified the proposed new formation mechanism of $CaO\text{-}SiO_2\text{-}Al_2O_3\text{-}(MgO)$ inclusions.

ACKNOWLEDGMENTS

Sincere gratitude and appreciation should be expressed by the authors to Xingtai Iron and Steel Corp., Ltd. for supporting of the research and great help during industrial samplings.

REFERENCES

1. L. Peeters: *Wire J. Int*., 1980, vol. 13, pp. 96–99.
2. E.G. Demeye: *Wire J. Int*., 1981, vol. 14, pp. 72–77.
3. M. Barous and G. Mangel: *Wire J. Int*., 1984, vol. 17, pp. 66–71.
4. C. Gatellier, H. Gaye, J. Lehman, J. Bellot, and M. Moncel: *Rev. Metall. Cah. Inf. Tec*., 1992, vol. 89, pp. 361–69.
5. G. Bernard, P.V. Ribound, and G. Urbain: *Rev. Metall. Cah. Inf. Tec*., 1981, vol. 78, pp. 421–34.
6. K. Iemura, H. Ichihashi, A. Kawami, and M. Mizutani: *Proc. of the 3th Int. Conf. on Clean Steel*., Brookfield. 1986, pp. 160–67.
7. S. Maede, T. Soejima, T. Saito, H. Matsumoto, H. Fujimoto, and T. Mimura: *72nd Steelmaking Conf. Proc*., Chicago. 1989, pp. 379–85.
8. K. Karihara: *Kobelco Technol. Rev*., 2011, vol. 30, pp. 62–65.
9. Y. Shinsho, T. Nozaki, K. Sorimachi, E. Yamanaka, K. Suzuki, and K. Nakanishi: *Wire J. Int*., 1988, vol. 21, pp. 145–53.
10. H. Ohta and H. Sutio: *Metall. Mater. Trans. B*, 1996, vol. 27, pp. 263–70.
11. H. Suito and R. Inoue: *ISIJ Int*., 1996, vol. 36, pp. 528–36.
12. G.M. Fauling: *Iron Steelmaker*, 1999, vol. 26, pp. 29–36.
13. D.H. Woo, Y.B. Kang, and H.G. Lee: *Metall. Mater. Trans. B*, 2002, vol. 33B, pp. 915–20.
14. Y.B. Kang and H.G. Lee: *ISIJ Int*., 2004, vol. 44, pp. 1006–15.
15. S.H. Chen, M. Jiang, X.F. He, and X.H. Wang: *Int. J. Miner. Metall. Mater*., 2012, vol. 19, pp. 490–98.
16. J.D. Seo, Y.T. Kim, and D.H. Kim: *5th Int. Congress on the Sci. and Technol. of Steelmaking*, Dresden, German. 2012. pp. 1250–54.
17. J.S. Park and J.H. Park: *Metall. Mater. Trans. B*, 2014, vol. 45B, pp. 953–60.
18. C.B. Guo, H.T. Ling, L.F. Zhang, C. Liu, G.S. Wang, and Y.B. GAO: *6th Int. Congress Sci. Technol. Steelmaking*, Beijing. 2015. pp. 817–20.
19. A. Ueno, K. Kimura, A. Kawami, and M. Mizutani: *70th Steelmaking Conf. Proc*., 1987. pp. 389–95.
20. E. Stampa and M. Cipparrone: *Wire J. Int*., 1987, vol. 20, pp. 44–55.
21. X.H. Wang, X.G. Li, F.X. Huan, H.B. Li, and J. Yang: *Steel Res. Int*., 2014, vol. 85, pp. 155–63.
22. A.W. Cramb and M. Byrne: *67th Steelmaking conf. proc*., Chicago. 1984, pp. 5–13.
23. M. Byrne, A.W. Cramb, and T.W. Fenicle: *Trans. ISS*, 1989, vol. 10, pp. 51–60.